Pharmaceutical Research, Vol. 13, No. 10, 1996

Research Article

Pharmacokinetic Analysis of Drug Disposition After Intratumoral Injection in a Tissue-Isolated Tumor Perfusion System

Akira Saikawa,[1] Takehiko Nomura,[1] Fumiyoshi Yamashita,[1] Yoshinobu Takakura,[1] Hitoshi Sezaki,[2] and Mitsuru Hashida[1,3]

Received January 25, 1996; accepted July 3, 1996

Purpose. The purpose of this study was to establish an experimental system for evaluation of the intratumoral behavior of drugs after intratumoral injection using perfused tissue-isolated tumor preparations of Walker 256 carcinoma (3.46–9.73g, n = 16). ***Methods.*** We quantified the recovery of Phenol Red (model drug) in the tumor, leakage from the tumor surface and the venous outflow after intratumoral injection using perfused tissue-isolated tumors, and analyzed venous appearance curves based on a pharmacokinetic model in which the tumor tissue was assumed to be divided into two compartments, i.e., well- and poorly-perfused regions. ***Results.*** In small tumors (Type 1, 5.42 ± 0.39 g), the drug appeared immediately in the venous outflow, and the amount remaining in the tumor tissue at 2 hr after injection was small. In contrast, the venous appearance rate reached a significantly lower peak a few minutes after injection, and a large amount of injected drug remained in some large tumors (Type 2, 8.17 ± 0.51 g). Pharmacokinetic analysis revealed that there was a correlation between tumor weight and the rate constants of transfer from the poorly-perfused region to the well-perfused region, and between the rate constants of transfer from the well-perfused region to the venous outflow and dosing ratios into the well-perfused region. ***Conclusions.*** An experimental system and analytical method were established for the evaluation of the intratumoral behavior of drugs after intratumoral injection using a tissue-isolated tumor perfusion system. This experimental system will be useful in analyzing the antitumor drug disposition after intratumoral injection.

KEY WORDS: pharmacokinetics; tissue-isolated tumor; intratumoral injection; drug disposition; perfusion experiment.

INTRODUCTION

In cancer therapy, intratumoral injection is an effective way to maximize the action of injected substances at the tumor site, while minimizing their systemic exposure (1). Intratumoral injection has been employed to deliver to the target tumor site substances such as antitumor drugs (2–4), bacteria components (5–7), cytokines (8–9), antisense oligonucleotides (10,11), and genes (12). However, there is little information on the disposition characteristics of the injected materials after intratumoral injection.

The "tissue-isolated" tumor preparation, originally developed by Gullino and Grantham (13) is a unique and useful experimental model system in cancer research. This model system is composed of a solid tumor with an artery and a vein, and the local disposition events occurring in the tumor tissue such as extravasation, interstitial diffusion, and tissue binding can be observed and independently evaluated. The system has been applied to elucidate the physiological properties of solid tumors such as blood flow (14,15), interstitial pressure (16,17), and energy metabolism (18). We previously established a perfusion experimental system using a tissue-isolated preparation of Walker 256 carcinoma for the evaluation of drug disposition in the tumor after intra-arterial injection. The pharmacokinetic properties of anticancer drugs and macromolecules after intra-arterial injection were clarified in relation to their physicochemical characteristics (19,20).

The first objective of the present study was to establish a method for the evaluation of drug disposition characteristics in solid tumors after intratumoral injection by applying this experimental model system. The second aim of the study was to reveal the mechanisms underlying the drug disposition after intratumoral injection. Based on the experimental data in this study, we designed a pharmacokinetic model in which the tumor tissue was separated into two regions, well- and poorly-perfused

[1] Department of Drug Delivery Research, Faculty of Pharmaceutical Sciences, Kyoto University, Sakyo-ku, Kyoto 606-01, Japan.
[2] Department of Pharmaceutics, Faculty of Pharmaceutical Sciences, Setsunan University, Osaka 573-01, Japan.
[3] To whom correspondence should be addressed.

ABBREVIATIONS: PR, phenol red; EB, Evans blue; BSA, bovine serum albumin; EB/BSA, bovine serum albumin labeled with Evans blue; VRS, vascular reference substance.

0724-8741/96/1000-1438$09.50/0

regions. Using this model, we analyzed two types of venous outflow patterns to derive the pharmacokinetic parameters which characterize intratumoral drug disposition.

MATERIALS AND METHODS

Chemicals

Evans blue (EB) and phenol red (PR) were purchased from Nacalai Tesque, Kyoto, Japan. Bovine serum albumin (BSA) (Fraction V) was obtained from Armour Pharmaceutical Co., U.K. All other chemicals were obtained commercially as analytical grade reagents.

Animals and Tumors

Female SLC Wistar rats weighing 100 to 130 g were obtained from Shizuoka Agricultural Association for Laboratory Animals, Shizuoka, Japan. The Walker 256 carcinoma was kindly supplied by Shionogi & Co., Osaka, Japan, and was maintained in rats by subcutaneous inoculation into neck every 2 weeks.

Perfusion of Tissue-Isolated Tumors

According to the method of Gullino (13,14), the tissue-isolated tumor was prepared as reported previously (Fig. 1) (20,21). About 10–14 days after tumor inoculation, tumors weighing 3–10 g were used for the perfusion experiment. In brief, rats were anesthetized with pentobarbital (40 mg/kg, i.p.) and, after a midline incision was made, all blood vessels supplying nontumorous tissues around the tumor (left renal artery and vein, left adrenal artery and vein, inferior vena cava, aorta and other collateral vessels) were ligated. The inferior vena cava and aorta were cannulated with vinyl tubings and perfused by maintaining tumor arterial pressure at 40–80 mmHg by adjusting the perfusate flow rate (about 0.8 ml/min). The perfusion medium was Tyrode's solution; a mixture of 137 mM NaCl, 2.68 mM KCl, 1.80 mM $CaCl_2$, 11.9 mM $NaHCO_3$, 0.362 mM NaH_2PO_4, 0.492 mM $MgCl_2$, and 5.55 mM D-glucose, containing bovine serum albumin (BSA) at a concentration of 4.7% (w/v), oxygenated with 95% O_2 – 5% CO_2 and adjusted to pH 7.4 maintained at 37°C. The viability of the perfused tumor was confirmed by measurement of the lactic acid production and the reestablishment of tumor growth after the perfusion experiment as reported previously (20). The isolated tumor was transferred on a petri dish to collect the fluid leaked out of the tumor surface during the intratumoral injection experiments (Fig. 1).

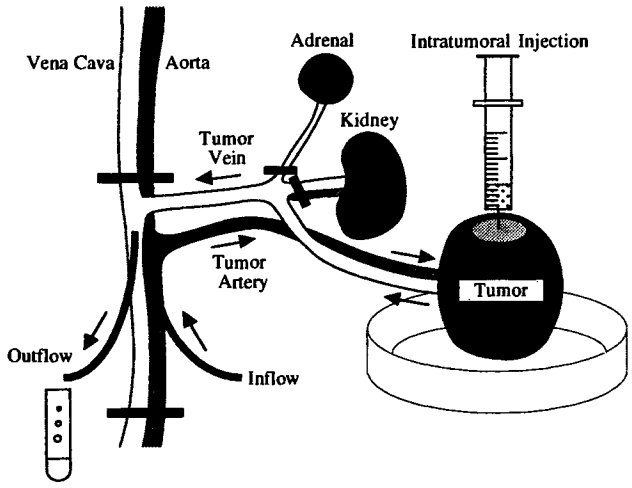

Fig. 1. Perfusion system of the tissue-isolated tumor preparation.

Indicator Dilution Experiment

To obtain the basic physiological information for the tumor preparation, indicator dilution experiments were carried out as reported previously (19) for 9 of the 16 tumors tested in the present study, prior to the intratumoral injection experiment. Briefly, BSA labeled with Evans blue (EB/BSA; EB: 2.0 mg/ml, BSA: 4.7%) as a vascular reference substance (VRS) was applied from the arterial side of the tumor by using a six-position valve injector (0.1 ml) as a pulse function. The outflow perfusate was collected into preweighed tubes at appropriate time intervals (initial interval 5 sec, subsequently 10–15 sec). The sample volume was calculated from the gain in weight of the tube by assuming the density of the perfusate to be 1.0. The sample was subjected to assay after an appropriate dilution with the perfusion buffer. The concentration was determined by using a spectrophotometer setting at 620 nm. Dilution curves were analyzed using moment analysis, and the statistical moment parameters were calculated as follows (21):

$$AUC = \int_0^\infty C dt \tag{1}$$

$$MTT = \int_0^\infty tCdt/AUC \tag{2}$$

where t is time and C is the concentration of EB/BSA normalized by injection dose with a dimension of percentage of dose/ml. AUC and MTT are the area under the concentration-time curve and the mean transit time, respectively. Taking into account the contribution of the catheters to the mean transit time in the tumor, all MTT values were corrected by subtracting the time corresponding to the transit through afferent and efferent tubes. The vascular volume of the tumor is calculated as follows:

$$V_T = Q \cdot MTT \tag{3}$$

where V_T and Q are the vascular volume of the tumor and the inflow rate, respectively.

Intratumoral Injection Experiment

Twenty minutes after the indicator dilution experiment, a solution of PR (100 μl, 10 mg/ml) in phosphate-buffered saline (pH 7.4) was injected over 30 sec into the center of the tumor. The injection point was covered with a Sealon film (about 1 cm diameter) which was attached to the injection needle with surgical adhesive (Aron Alpha, Sankyo Co., Tokyo, Japan), and the injection needle was left imbedded in the tumor during the perfusion experiment to prevent fluid leakage from the injection site. The venous effluent was collected into preweighed tubes for 120 min, at appropriate time intervals (initial interval 1 min, subsequently 2–6 min). A constant arterial pressure was maintained during the intratumoral injection experiment. The

sample volume was calculated from the gain in weight of the tube by assuming the density of the perfusate to be 1.0. At the end of infusion, the tumor was excised and subjected to macroscopic observation by cutting the tissue in halves; the tumor tissues were then homogenized, diluted with a mixture of acetone/water (2:1 w/w, three times the volume of the tumor), and centrifuged (3000 rpm × 2, 10 min), and the supernatant containing PR was collected. The supernatant was diluted with 2N NaOH and subjected to UV assay at 560 nm. The measurement was done immediately after the addition of NaOH to avoid fading. Outflow perfusate prior to the injection of PR was used for the subtraction of blank absorbance values. At the end of the experiment, the fluid which had leaked out of the tumor surface during the 120 min perfusion on the petri dish was collected and subjected to the assay.

Pharmacokinetic Analysis

The venous appearance curves of the drugs injected were analyzed based on a pharmacokinetic model shown in Fig. 3. In this model, the tumor tissue is assumed to be composed of

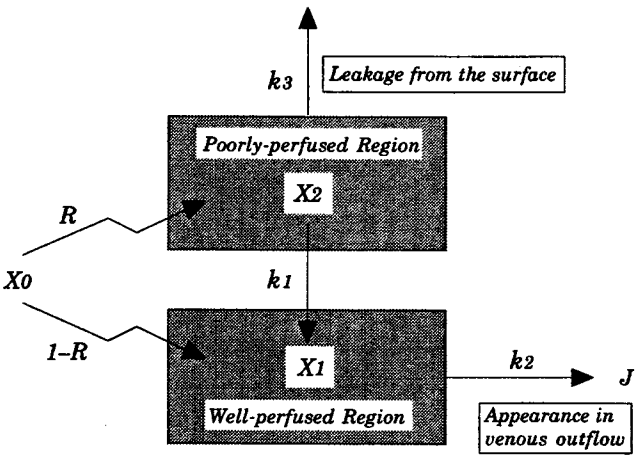

Fig. 3. Pharmacokinetic model for analysis of drug disposition after intratumoral injection. k_1, rate constant of transfer from poorly-perfused region to well-perfused region; k_2, venous appearance rate constant; k_3, rate constant of leakage from the surface; R, dosing ratio into poorly-perfused region; X_0, injected dose; X_1, drug amount in well-perfused region; X_2, drug amount in poorly-perfused region; J, appearance rate in venous outflow.

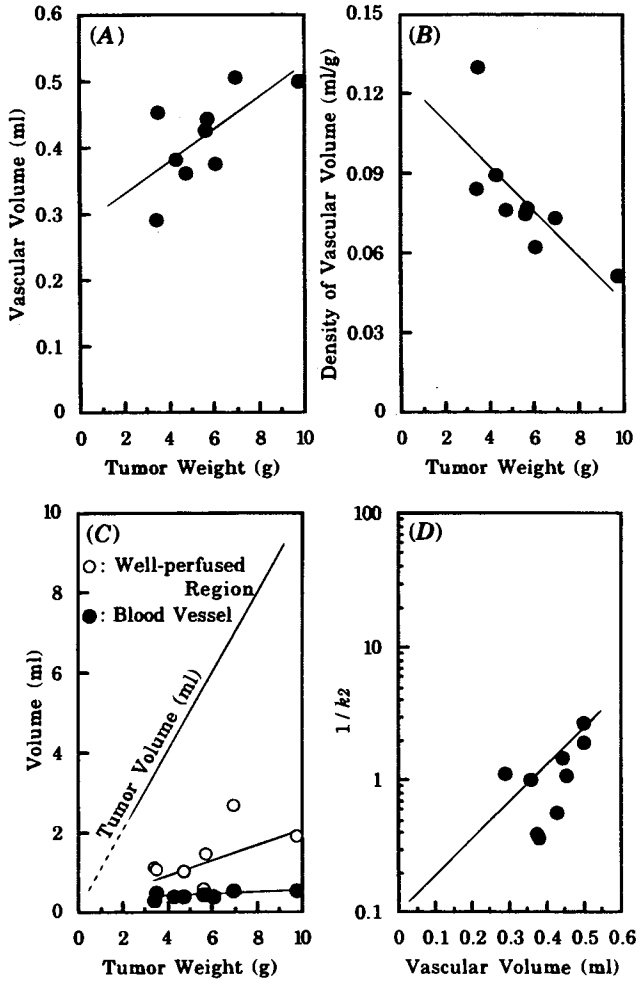

Fig. 2. Relation between tumor weight and vascular volume (*A*), density of vascular volume (*B*) and volume of well-perfused region (*C*). Relation between vascular volume and k_2 (*D*). Tumor volume (*C*) was calculated from the tumor weight by assuming the density of the tumor to be 1.0.

two compartments, well-perfused and poorly-perfused regions. Drugs in the well-perfused region are assumed to be cleared from the vascular side quickly and those in the poorly-perfused region are assumed to be transferred to the well-perfused region or to leak out. The poorly-perfused region is assumed to have little blood supply and also to contain some necrotic tissue. The well-perfused region, in contrast, is assumed to consist of vascular space and its surrounding space, which is in equilibrium to the vascular space. Based on this model, the following equations were derived to describe the change in drug amount in these two regions with time.

$$\frac{dX_1}{dt} = k_1X_2 - k_2X_1 \tag{4}$$

$$\frac{dX_2}{dt} = -(k_1 + k_3)X_2 \tag{5}$$

where X_1 and X_2 are the drug amounts in the well- and poorly-perfused regions (% of dose), respectively; k_1 is the rate constant of transfer from the poorly-perfused region to the well-perfused region (/min); k_2 is the venous appearance rate constant (/min); and k_3 is the rate constant of leakage from the surface (/min). The integration of Equations [4] and [5] gives

$$J = Ae^{-\alpha t} + Be^{-\beta t} \tag{6}$$

$$A = k_2X_0\frac{k_1 + (1 - R)(k_3 - k_2)}{k_1 + k_3 - k_2} \tag{7}$$

$$B = -\frac{k_1k_2RX_0}{k_1 + k_3 - k_2} \tag{8}$$

$$\alpha = k_2 \tag{9}$$

$$\beta = k_1 + k_3 \tag{10}$$

where J is the appearance rate in venous outflow, which is equal to k_2X_2 (% of dose/min); X_0 is the injected dose (100%); and R is the dosing ratio into the poorly-perfused region. The venous outflow pattern for each tumor preparation was then fitted to Equation [6] by using the nonlinear regression program MULTI (22) to estimate the pharmacokinetic parameters.

RESULTS

Indicator Dilution Experiment

Regardless of the enhanced vascular permeability in tumor tissue, the uptake of EB/BSA by the tissue-isolated tumor was negligible during a single passage of the tumor preparation, and almost 100% of injected EB/BSA was recovered in the venous outflow (data not shown). The outflow concentration-time curve was analyzed by moment analysis to obtain the vascular volume of the tumor (V_T, equation [3]). V_T of EB/BSA corresponds to the apparent vascular volume of tumor tissue preparation. The vascular volume of the tissue-isolated Walker 256 carcinomas used in this study were in the range of 0.065 to 0.1 ml/g in the weight range of 3.46 to 9.73 g, and vascular volume (ml) increased as tumor weight increased (Fig. 2, A). However, the density of vascular space (ml/g) decreased with an increase in tumor weight (Fig. 2, B). These values are in good agreement with the values reported previously in isolated tumor preparations (19). Song and Levitt (23) also reported that the average vascular volume of s.c.-implanted Walker 256 carcinomas was 0.079 ml/g, and that this volume decreased linearly with tumor size, using ^{51}Cr-labeled erythrocytes. These findings confirm the validity of our present tumor preparations.

Appearance of PR in Venous Outflow After Intratumoral Injection

Figure 4 shows the venous appearance curves of PR after intratumoral injection. In small tumors (Type 1, mean weight ± SE; 5.42 ± 0.39 g, n = 12), PR appeared immediately in the venous outflow and the pattern was biphasic, whereas in some large tumors (Type 2, 8.17 ± 0.51 g, n = 4), the venous appearance rate reached a lower peak in a few minutes after injection and then decreased slowly.

Recovery of PR in Outflow, Extruded Fluid, and Tumor Tissue After Intratumoral Injection

The recoveries of PR at 120 min after intratumoral injection in the 16 tumors are shown in Figure 5, and the mean recoveries are summarized in Table I. In Type 1 tumors (n = 12), a large amount of injected drug was recovered in the venous outflow (61.60 ± 8.61% of dose), and the amount remaining in the tumor tissue was small (9.02 ± 2.62% of dose). In contrast, the amount of the drug remaining in Type 2 tumors (n = 4) was significantly larger (31.33 ± 8.94% of dose) and that in the venous outflow perfusate was much smaller (26.70 ± 8.94% of dose) than that observed for the Type 1 tumors. The amount of the drug leaked from the tumor varried greatly among the tumor tissues tested, and no significant difference was observed between the amounts of drug leakage from the surface of Type 1 and Type 2 tumors. However, as shown in Figure 5, the recovery of PR in the leakage from the tumor surface had a tendency to increase as the tumor weight increased.

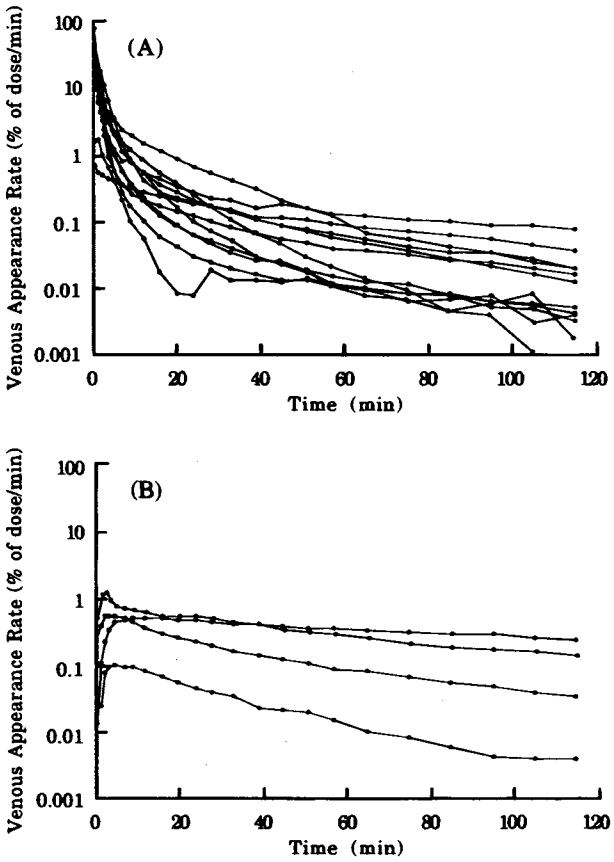

Fig. 4. Venous appearance curves of PR after intratumoral injection into tissue-isolated perfused tumors. (A) Type 1 tumors (5.42 ± 0.39 g, n = 12), (B) Type 2 tumors (8.17 ± 0.51 g, n = 4).

Pharmacokinetic Analysis

Table II summarizes the pharmacokinetic parameters obtained in this study. The rate constant of transfer from the poorly-perfused region to the well-perfused region (k_1) and the dosing ratio into the poorly-perfused region (R) of Type 1 tumors were significantly different from those of Type 2 tumors. No great difference was observed between the venous appearance rate constants (k_2). The rate constants of leakage from the surface (k_3) of Type 1 and Type 2 tumors were 0.057 ± 0.019/min (0.000–0.188, n = 12) and 0.018 ± 0.008/min (0.001–0.037, n = 4), respectively.

DISCUSSION

Solid tumor tissues are known to have elevated interstitial pressure (17,24,25) and randomly distributed microvessels (26,27). In addition, fluid regularly oozes out of the tumor surface (28). In the present study, Sealon film was attached to the injection needle with bond, and the needle was left imbedded in the tumor during perfusion to prevent fluid leakage from the injection site after intratumoral injection. We measured drug concentrations in the perfusates from both venous outflow and leakage from the tumor surface and in the tumor tissue for

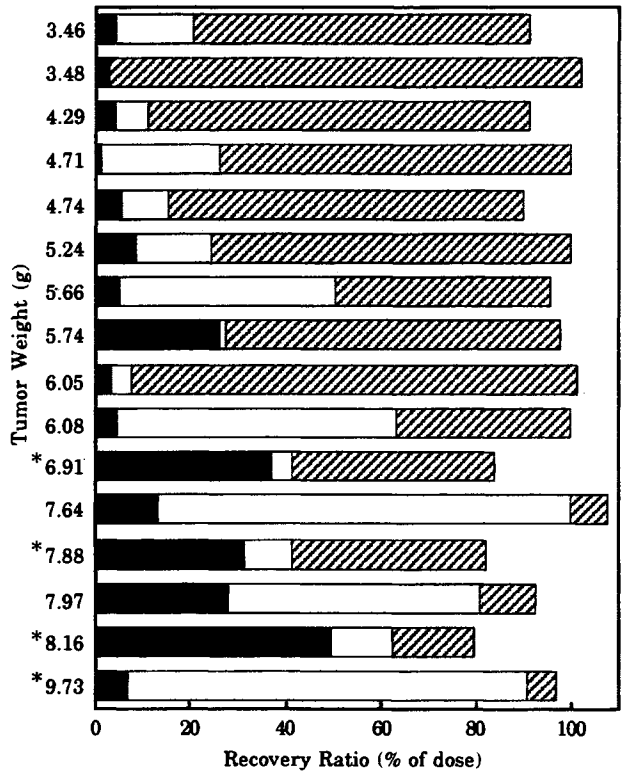

Fig. 5. Recovery ratios of phenol red at 2 h after intratumoral injection into 16 tissue-isolated perfused tumors. ■, remaining in tumor tissue; □, leakage from surface of tumor; ▨, recovery in venous outflow. *; Type 2 tumors.

Table I. Recoveries of Phenol Red 2 hr After Intratumoral Injection in Perfused Tissue-Isolated Tumors

	Recoveries (% of dose)		
Tumor	venous outflow*	leakage from the surface	tumor tissue*
Type 1	61.60 ± 8.61	26.95 ± 7.99	9.02 ± 2.62
Type 2	26.70 ± 8.94	27.78 ± 18.74	31.33 ± 8.94

Note: Results are expressed as the mean ± SE. There is a significant difference between Type 1 and Type 2 tumors by Student's t test:(*) $P < 0.001$.

quantitative analysis. The mean amount of fluid loss from the tumor surface during the 2 hr perfusion experiments was about 6% of the perfusates entering the tumor. This value is in good agreement with the reported values of an interstitial fluid loss *in vivo* which are usually in the range of 6–14% of the plasma entering the tumor which oozes out into the surrounding normal tissue (28,29).

The recovery in the venous outflow for Type 1 tumors was significantly larger than that for Type 2 tumors (Table I), while the remaining PR in Type 1 tumor tissues was smaller than that in Type 2 tumor tissues. There was no significant difference between the recoveries in leakage from the surface of Type 1 and Type 2 tumors. These results suggest that there are anatomical and physiological differences between small (Type 1) and large (Type 2) tumors. In large tumors, the drug injected in the centre of the tumor, which is usually poorly perfused and may contain necrotic regions, would be transported slowly to the well-vascularized region. In small tumors, the centers of tumors are comparatively well-vascularized, and the injected drug would appear rapidly in the venous outflow. It is also reported that interstitial pressure was the highest in the center of tumors and decreased toward the periphery, and there is a strong correlation between the mean interstitial pressure and the mass of the tissue-isolated tumor for Walker 256 carcinosarcoma (17). Large tumors have relatively higher interstitial pressure than small tumors, and hence much of the interstitial fluid can easily ooze out of the tumor surface; however, the leakage from the surface of the present tested isolated tumors was considered to be based upon the anatomical characteristics of each tumor preparation.

In this study, we classified the tumors into two types according to the outflow patterns. The recovery ratio of each tumor preparation shown in Figure 5 indicates that there are some Type 1 tumors that have anatomical characteristics which can be classified as those of Type 2 tumors. Since the outflow patterns depend strongly on the anatomical characteristics at the injection sites, when drugs are injected into relatively a well-perfused region, some "anatomically Type 2 tumors" show outflow patterns like those of Type 1 tumors. There were some Type 1 and Type 2 tumors which showed large recovery in tumor tissue and venous outflow, respectively (Fig. 5).

To characterize the intratumoral behavior of injected substances, pharmacokinetic analysis was carried out against outflow concentration-time curves. Since all the venous outflow patterns were biphasic, we constructed a simple two-compartment model as described in the Materials and Methods section. In this model, tumor tissue was assumed to be divided into two compartments, well- and poorly-perfused regions.

Based upon this model, the venous appearance curves of injected drug were analyzed and pharmacokinetic parameters

Table II. Pharmacokinetic Parameters of Phenol Red After Intratumoral Injection

		Pharmacokinetic parameters			
Tumor	Weight (g)	$k1$ (min^{-1})*	$k2$(min^{-1})	$k3$(min^{-1})	R*
Type 1	5.42 ± 0.39	0.039 ± 0.012	1.24 ± 0.22	0.057 ± 0.019	0.54 ± 0.085
Type 2	8.17 ± 0.51	0.0043 ± 0.0013	0.54 ± 0.18	0.018 ± 0.0083	0.99 ± 0.011

Note: Type 1: The drug appeared immediately in the venous outflow and its appearance rate decreased quickly. Type 2: The venous appearance rate reached a significantly lower peak in a few minutes and then decreased slowly. Results are expressed as the mean ± SE. There is statistically significant difference between Type 1 and Type 2 tumors by Student's test: (*) $P < 0.001$.

were estimated and listed as mean values in Table II. We further evaluated the pharmacokinetic parameters for each tumor preparation in detail and found correlations between tumor weight and some pharmacokinetic parameters. Figure 6 shows the relation between tumor weight and k_1, k_2, k_3 or R. The reciprocal value of k_1 increased as tumor weight increased. This phenomenon can be mathematically described by the following equation, which illustrates that the value of transfer clearance from the poorly-perfused region to the well-perfused region decreases, or the volume of the poorly perfused-region increases, as the reciprocal value of k_1 increases.

$$\frac{1}{k_1}\,(\text{min}) = \frac{\text{Volume of poorly-perfused region (ml)}}{\text{Transfer clearance (ml/min)}}$$

Transfer clearance from the poorly-perfused region to the well-perfused region involves diffusion and convection. There is not so much difference in the diffusibility of PR in the tissue of each tumor preparation, and convective flow is considered to be relatively constant because the inflow rate in each tumor preparation was maintained at an almost constant rate (0.8 ml/min) in this study. The volume of poorly-perfused region is thought to significantly increase as the tumor weight increases because of the formation of central necrosis. In light of this, the wide variation in the value of $1/k_1$ is considered to be caused by the variation in the volume of poorly-perfused region.

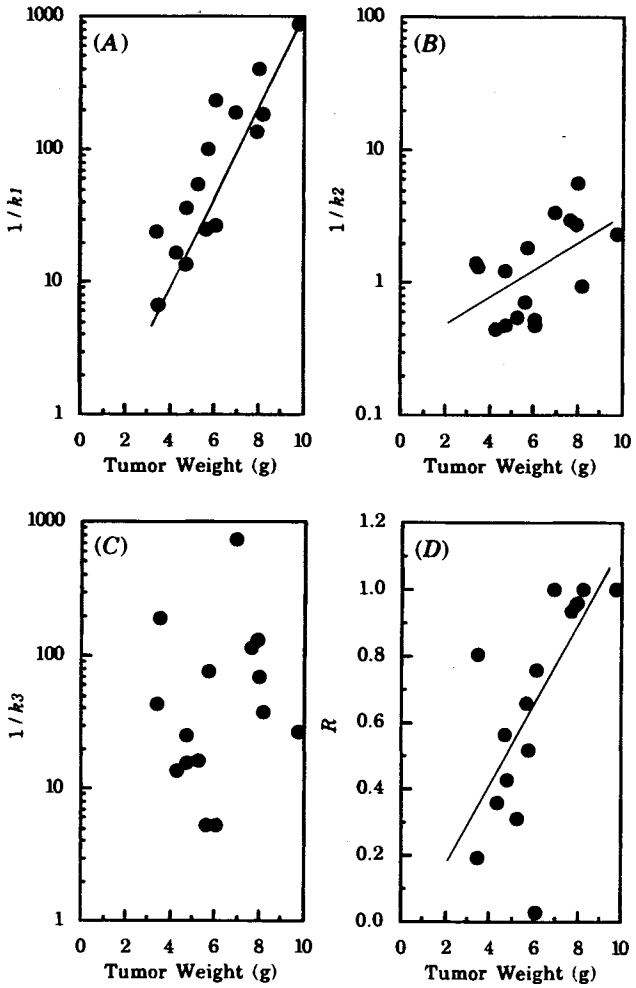

Fig. 6. Relation between tumor weight and rate constant of transfer from the poorly-perfused region to the well-perfused region, k_1 (*A*); rate constant of venous appearance, k_2 (*B*); rate constant of leakage from the surface, k_3 (*C*); dosing ratio into the poorly perfused region, R (*D*).

The reciprocal value of k_2 slightly increased as the tumor weight increased ($r = 0.533$). The value of k_2 is defined by the following equation,

$$\frac{1}{k_2}\,(\text{min}) = \frac{\text{Volume of well-perfused region (ml)}}{\text{Clearance into venous outflow (ml/min)}}$$

Since the clearance into the venous outflow of each tumor preparation is almost equal to the outflow rate (constant), the value of k_2 should correspond to the volume of the well-perfused region, which is considered to correlate to the vascular volume.

Based on this assumption, the vascular volume and the volume of the well-perfused region, which is calculated by dividing Q with k_2, were plotted against tumor weight as shown in Figure 2, (*C*), showing that both the volume of the well-perfused region and vascular volume increase as the tumor weight increases. Thus, the value of $1/k_2$ also correlates to the vascular volume as shown in Figure 2, (*D*).

The volume of the well-perfused region was greater than the intravascular volume but smaller than the tumor volume (Figure 2, (*C*)). These results suggest that, in this model, the well-perfused region actually corresponds to intravascular space and its surrounding space, which is in equilibrium to the intravascular space.

The value of k_3 did not correlate with tumor weight, suggesting that the leakage from the tumor surface varies from tumor to tumor and depends largely on the pressure during the intratumoral injection and the anatomical characteristics of each injection site. In large tumors, where the center region of the tumor is usually the necrotic area, the value of R increased with the tumor weight ($r = 0.683$), approaching almost 1, indicating that almost all drug molecules were injected into the poorly-perfused region.

The values of k_2 for both types of tumor were about 30–100 times larger than those of k_1. This indicates that the dominant process which determines the retention time of the drug in the tumor is not the venous appearance rate (k_2) but the rate of transfer from the poorly-perfused region to the well-perfused region (k_1), and it may be possible to classify the tumors into two types (1,2) based on the value of k_1. In this way, we could evaluate each intratumoral transfer rate separately by this pharmacokinetic analysis.

It is difficult to explain this pharmacokinetic model clearly relative to actual tumor anatomy. In consideration of both the general characteristics of tumor anatomy as mentioned above and the observation of this study, the well-perfused region is considered to correspond to intravascular space, and its surrounding spaces (which is in equilibrium to intravascular space); and the poorly-perfused region corresponds to other areas with no blood supply which may consist mainly of necrotic tissue. The appearance in the venous outflow of drugs injected into the poorly-perfused region would be delayed by the slow rate process represented by the value of k_1. The leakage process of PR from the tumor surface after intratumoral injection is considered to be associated mainly with the poorly-perfused region. This assumption would be supported by the following

experimental evidence. The first is that leakage of EB/BSA and other low molecular weight drugs from the tumor surface was not observed after intraarterial injection (19). Most of the drug (PR) appearing in the vascular side after intratumoral injection did not leak and be recovered in the venous outflow quickly. The second is that, in these tumor preparations, necrotic areas which were connected to the central necrotic tissues were found in the periphery of the tumor, and apparent fluid leakage could be observed mainly from those areas. It is reasonable to assume that the drug leakage occurred mainly from the injection site through those areas. Although distribution of these peripheral necrotic areas was heterogeneous and varied largely between tumor preparations, these areas tended to increase as the tumor weight increased.

In previous tissue perfusion experiments, BSA is often added to the perfusate to maintain colloidal osmotic pressure, and may affect the disposition of the injected drug, especially with a high protein-binding property (30). In the present study, isolated tumors were perfused with 4.7% BSA, and the binding percentage of PR with BSA in the perfusate is about 90%. In our preliminary study, mitomycin C (*Mr*; 334), whose binding percentage with BSA is only about 10% in this perfusion system, showed behavior similar to that of PR after intratumoral injection. This indicates that the effect of protein binding on this perfusion experiment is relatively small for low molecular weight drugs. In this sense, similar results will be obtained in the case of typical marker substances such as sucrose (*Mr*; 342) and probably water.

The present study established and demonstrated the methodology of experiments and pharmacokinetic analysis for the basic disposition of drugs after intratumoral injection. This technique will be useful for the evaluation of the tumor disposition of various therapeutic agents such as antitumor drugs, cytokines, antisense oligonucleotides, and genes after intratumoral injection.

ACKNOWLEDGMENTS

This work was supported in a part by a Grant-in-Aid for Scientific Research from the Ministry of Education, Science, and Culture, Japan.

REFERENCES

1. Y. Takakura and M. Hashida. *Critical Reviews in Oncology/Hematology* **18**:207–231 (1995).
2. M. Hashida, A. Kato, T. Kojima, S. Muranishi, H. Sezaki, N. Tanigawa, K. Satomura and Y. Hikasa. *Gann* **72**:226–234 (1981).
3. W. A. Knepp, A. Jayakrishman, J. M. Quigg, H. S. Sitren, J. J. Bagnall and E. P. Goldberg. *J. Pharm. Pharmacol.* **45**:887–891 (1993).
4. J. E. Landrito, K. Yoshiga, K. Sakurai and K. Takada. *Anticancer Res.* **14**:113–118 (1994).
5. B. Zbar, I. D. Bernstein, G. L. Bartlett, Jr. M. G. Hanna and H. J. Rapp. *J. Natl. Cancer Inst.* **49**:119–130 (1972).
6. C. A. McLaughlin, J. L. Cantrell, E. Ribi and E. P. Goldberg. *Cancer Res.* **38**:1311–1316 (1978).
7. J. Kanellos, I. F. C. Mckenzie and G. A. Pietersz. *Immunol. Cell Biol.* **67**:89–99 (1989).
8. L. T. M. Balemans, V. Mattijssen, P. A. Steerenberg, B. E. M. Van Driel, P. H. M. De Mulder, and W. Den Otter. *Cancer Immunol. Immunother.* **37**:7–14 (1993).
9. T. Ebina, K. Murata and K. Tamura. *Jpn. J. Cancer Res.* **85**:93–100 (1994).
10. I. Kitajima, T. Shinohara, T. Minor, L. Bibbs, J. Bilakovics and M. Nerenberg. *J. Biol. Chem.* **267**:25881–25888 (1992).
11. M. Z. Ratajczak, J. A. Kant, S. M. Luger, N. Hijiya, J. Zhang, G. Zon and A. M. Gewirtz. *Proc. Natl. Acad. Sci. USA* **89**:11823–11827 (1992).
12. G. E. Plautz, Z. Yang, B. Wu, X. Gao, L. Huang and G. J. Nabel. *Proc. Natl. Acad. Sci. USA* **90**:4645–4649 (1993).
13. P. M. Gullino and F. H. Grantham. *J. Natl. Cancer Inst.* **27**:679–693 (1961).
14. P. M. Gullino. In: BUSCH, H. (eds.) *Methods in Cancer Research*, Academic Press, New York, 1970, pp. 45–91.
15. E. G. Kristjansen Paul, S. Roberge, I. Lee, and R. K. Jain. *Microvascular Research* **48**:389–402 (1994).
16. E. M. Sevick and R. K. Jain. *Cancer Res.* **49**:3506–3512 (1989).
17. Y. Boucher, L. T. Baxter and R. K. Jain. *Cancer Res.* **50**:4478–4484 (1990).
18. C. J. Eskey, A. P. Koretsky, M. M. Domach and R. K. Jain. *Proc. Natl. Acad. Sci. USA* **90**:2646–2650 (1993).
19. K. Ohkouchi, H. Imoto, Y. Takakura, M. Hashida and H. Sezaki. *Cancer Res.* **50**:1640–1644 (1990).
20. H. Imoto, Y. Sakamura, K. Ohkouchi, R. Atsumi, Y. Takakura, H. Sezaki and M. Hashida. *Cancer Res.* **52**:4396–4401 (1992).
21. T. Kakutani, K. Yamaoka, M. Hashida and H. Sezaki. *J. Pharmacokinet. Biopharm.* **13**:609–631 (1985).
22. K. Yamaoka, Y. Tanigawara, T. Nakagawa and T. Uno. *J. Pharmacobio. Dyn.* **4**:*879–885 (1981).*
23. C. W. Song and S. H. Levitt. *Cancer Res.* **31**:587–589 (1971).
24. R. K. Jain. *Cancer Res.* **48**:2641–2658 (1988).
25. R. Gutmann, M. Leunig, J. Feyh, A. E. Goetz, K. Messmer, E. Kastenbauer and R. K. Jain. *Cancer Res.* **52**:1993–1995 (1992).
26. R. K. Jain. *Cancer Metastasis Rev.* **6**:559–593 (1987).
27. R. K. Jain. *Cancer Res.* **47**:3039–3051 (1987).
28. T. P. Butler, F. H. Grantham and P. M. Gullino. *Cancer Res.* **35**:3084–3088 (1975).
29. R. K. Jain. In: B. TEICHER (eds.), *Drug resistance in oncology, New York*: Marcel Dekker. 1993.
30. E. Nara, T. Hatono, M. Hashida and H. Sezaki. *J. Pharm. Pharmacol.* **15**:272–274 (1991).